Properties of the Renormalized Random-Phase Approximation for Dilute Magnetic Alloys

D. R. HAMANN
Bell Telephone Laboratories, Murray Hill, New Jersey 07974
(Received 1 April 1969)

The Anderson model for dilute magnetic alloys is studied in the renormalized random-phase approximation recently applied to the Wolff model by Suhl and co-workers. The resulting integral equations are solved analytically in an approximation which treats the key logarithmic divergence correctly. The solution indicates that the characteristic temperature in this theory depends exponentially on $(U/\Delta)^2$, where U is the Coulomb interaction and Δ the d-level width. This shows that the Kondo effect is not properly included in the basic approximation.

I. INTRODUCTION

OUR understanding of dilute paramagnetic alloys has advanced along an entirely new path as a result of recent calculations by Suhl and co-workers.[1–3] They studied a model consisting of a band of interacting electrons and a local impurity potential. This model was shown by Wolff[4] to possess a magnetic instability in the Hartree-Fock approximation as the electron-electron repulsion approached a certain critical value depending on the impurity potential. Suhl reasoned that the large local spin fluctuations existing near this threshold would modify the effective impurity potential in such a manner that the threshold would never quite be reached.

Under even the simplest assumptions, corresponding to a renormalized random-phase approximation (RRPA), this idea translated into a set of two coupled nonlinear integral equations. These were solved by brute force numerical iteration. The resulting temperature-dependent magnetic susceptibilities and electrical resistivities bear a marked resemblence to the experimentally observed properties of a number of alloys.

In the course of exploring some of the interesting questions raised by this work, it seemed desirable to supplement the numerical results with an approximate analytic solution of the integral equations. Such a solution is reported here. Its most significant consequence bears on the conjectured relation between this theory[3] and the Kondo effect,[5] in which the characteristic temperature associated with this effect depends exponentially on the ratio of the electron repulsion to the impurity level width. The characteristic temperature appearing in the present work depends exponentially on the *square* of this same ratio, and is exponentially smaller than the Kondo temperature. This leads us to believe that the processes responsible for the Kondo scattering divergence are not included in Suhl's RRPA treatment. In the first two papers of the Suhl series,[1,2] this same opinion was expressed. That this theory included a mechanism similar to the Kondo effect was surmised only after the temperature dependence of the resistivity had been calculated.[3]

In the present work, the dilute alloy model introduced by Anderson[6] is studied rather than the very general model used by Suhl.[1] This choice was largely a matter of taste. After the set of Feynman diagrams to be summed is chosen, Suhl makes a series of simplifying assumptions that reduce his key equations to those which are obtained directly when one begins with Anderson's model. The Kondo effect for Anderson's model has been demonstrated in several ways,[7,8] and its connection with the s-d exchange model has been derived,[9] so expressing our results in terms of the parameters of this model should facilitate comparison with these and other studies.

In Sec. II, the coupled equations are derived from Anderson's model, and the sums over complex energies that occur are transformed into real-axis integrations. In Sec. III, the self-energy operator is examined in detail, and a series of approximations is introduced which bring Dyson's equation into a soluble form. The last paragraph of Sec. III presents a summary, and the remainder can be skipped without loss of continuity. The solution of this integral equation is given in Sec. IV. A transcendental equation remains, which is analyzed in Sec. V. In Sec. VI, the significance of the results is discussed.

II. GREEN'S-FUNCTION EQUATIONS

The Hamiltonian for Anderson's model is[6]

$$H=H_0+H_1,$$
$$H_0=\sum_{k\sigma}\epsilon_k n_{k\sigma}+\sum_{\sigma}\epsilon_d n_{d\sigma}+V\sum_{k\sigma}(C_{k\sigma}^{\dagger}C_{d\sigma}+C_{d\sigma}^{\dagger}C_{k\sigma}), \quad (1)$$
$$H_1=Un_{d\uparrow}n_{d\downarrow}.$$

We wish to treat this model by standard finite-temperature diagrammatic perturbation theory.[10] It is cus-

[1] H. Suhl, Phys. Rev. Letters **19**, 442 (1967).
[2] M. Levine and H. Suhl, Phys. Rev. **171**, 567 (1968).
[3] M. Levine, T. V. Ramakrishnan, and R. A. Weiner, Phys. Rev. Letters **20**, 1370 (1968).
[4] P. A. Wolff, Phys. Rev. **124**, 1030 (1961).
[5] J. Kondo, Progr. Theoret. Phys. (Kyoto) **32**, 37 (1964).
[6] P. W. Anderson, Phys. Rev. **124**, 41 (1961).
[7] D. J. Scalapino, Phys. Rev. Letters **16**, 937 (1966).
[8] D. R. Hamann, Phys. Rev. **154**, 596 (1967); J. A. Appelbaum, *ibid.* **165**, 632 (1968).
[9] J. R. Schrieffer and P. A. Wolff, Phys. Rev. **149**, 491 (1966).
[10] A. A. Abrikosov, L. P. Gor'kov, and I. E. Dzyaloshinski, *Methods of Quantum Field Theory in Statistical Physics*, translated by R. A. Silverman (Prentice-Hall, Inc., Englewood Cliffs, N. J., 1963).

tomary to diagonalize H_0 and work in the representation of its one-electron eigenstates. Rather than do this, we shall follow Schrieffer and Mattis,[11] who showed that by remaining in the $\mathbf{k}$-d representation, all $\mathbf{k}$ sums can be carried out *ab initio*, and one need only consider diagrams with the d propagator,

$$G_{d\sigma}^{0}(\epsilon)=1/(\epsilon-\epsilon_d\pm i\Delta). \tag{2}$$

We have taken the density of states to be a constant ρ and $\Delta=\pi\rho V^2$. The plus sign in Eq. (2) denotes the retarded propagator, and the minus sign the advanced. In the following, propagators should be understood to be retarded unless otherwise noted.

It is especially convenient to make a particular choice of parameters,

$$\epsilon_d=-\tfrac{1}{2}U. \tag{3}$$

When this is done, the Hamiltonian has complete particle-hole symmetry. The transformation relating the s-d exchange model to the Anderson model is perfectly well behaved at this point in parameter space,[9] as is the perturbation expansion.[7] There is a physical argument indicating that Eq. (3) is the best choice because the parameter ϵ_d represents the impurity potential. In a real metal, components of the Coulomb interaction neglected in this model will modify the potential through screening, and adjust it so that an integral number of extra electrons (or holes) surround the impurity. For a uniform density of states, the choice in Eq. (3) can be shown to require

$$\langle n_{d\sigma}\rangle=\tfrac{1}{2}, \tag{4}$$

$$\sum_{k\sigma}\langle n_{k\sigma}\rangle=N, \tag{5}$$

where N is the original number of conduction electrons. Thus, exactly one extra electron is added by the impurity.

Because of (4), the Hartree-Fock contribution to the self-energy can be calculated immediately, and is found to just cancel the real energy in $(G_{d\sigma}^{0})^{-1}$,

$$G_{d\sigma}^{\mathrm{HF}}(\epsilon)=1/(\epsilon+i\Delta). \tag{6}$$

Following Suhl,[1] we shall assume that the most important Boson-like mode in this system is described by the sum of diagrams which correspond to the susceptibility in the Hartree-Fock approximation, Fig. 1. When Eq. (6) is used for G_d in computing these sums,

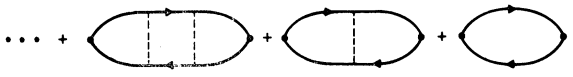

FIG. 1. Diagram sum for the susceptibility in the time-dependent Hartree-Fock or RPA. The solid lines are bare G_d propagators given by Eq. (6), and the dotted lines are the Coulomb repulsion in the d state, U.

[11] J. R. Schrieffer and D. C. Mattis, Phys. Rev. **140**, A1412 (1965).

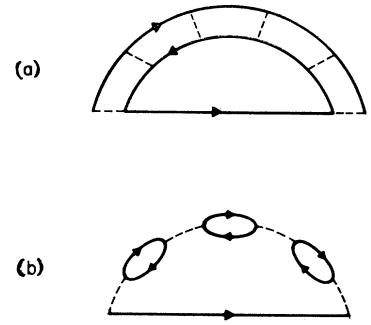

FIG. 2. The self-energy diagrams used. The sum over all ladder configurations in (a) and all bubble configurations in (b) is intended. The solid lines here are renormalized G_d's including these self-energy diagrams.

the susceptibility diverges for $U=\pi\Delta$. When G_d is renormalized by including the simplest self-energy diagram incorporating this Boson-like mode, Fig. 2, the sums in Fig. 1 remain finite for all U, but become large and strongly peaked at low frequency for $U>\pi\Delta$. Once such renormalized G_d's are used, the Fig. 1 diagrams no longer constitute a conserving approximation for the susceptibility, as discussed by Levine and Suhl.[2] Nevertheless, we shall use the symbol $\chi(\omega)$ for these diagrams, and hope that they give the most important contribution to the actual susceptibility.

The susceptibility for $U=0$ is just the first term in Fig. 1,

$$\chi_0(\omega)=-T\sum_n G_d(i\epsilon_n)G_d(\omega+i\epsilon_n), \tag{7}$$

where $\epsilon_n=(2n+1)\pi T$. The complete Fig. 1 sum is then

$$\chi(\omega)=\chi_0(\omega)/[1-U\chi_0(\omega)]. \tag{8}$$

The sum in (7) may be converted into a real-axis integral by standard methods.[10] We find

$$\chi_0(\omega)=-\frac{1}{2\pi}\int_{-\infty}^{\infty}d\epsilon\,\tanh\frac{\epsilon}{2T}\,\mathrm{Im}G_{dR}(\epsilon)\times[G_{dR}(\epsilon+\omega)+G_{dA}(\epsilon-\omega)], \tag{9}$$

where the subscripts R and A denote retarded and advanced propagators.

The self-energy, Fig. 2, is given by

$$\Sigma(\epsilon)=\tfrac{3}{2}U^2T\sum_n G_d(\epsilon-i\omega_n)\chi(i\omega_n), \tag{10}$$

where $\omega_n=2n\pi T$. Equation (10) does not include the Hartree-Fock term, which we have already taken into account. The set of equations which must be solved self-consistently is completed by Dyson's equation:

$$G_d(\epsilon)=1/[\epsilon+i\Delta-\Sigma(\epsilon)]. \tag{11}$$

Equations (10) and (11) correspond to Eq. (11) of Ref. 1 except for the numerical factor $\frac{3}{2}$. In Ref. 1,

the corresponding factor is $\frac{3}{4}$. In this work, a contribution 1 comes from the ladder diagrams, Fig. 1(a), and a contribution $\frac{1}{2}$ from the singular triplet part of the bubble diagrams, Fig. 1(b). Iteration of the square interaction vertices used in Ref. 1 generates both ladders and bubbles. However, only one of the two possible particle-hole channels defined for square vertices was used for iteration there, and the additional ladders and bubbles generated by iterating the other way were neglected. The correction of this factor does not change the results qualitatively.

It will also be necessary to have the sum in Eq. (10) represented by a real-axis integral, and it proves convenient to divide this into three terms:

$$\Sigma(\epsilon)=\Sigma_1(\epsilon)+\Sigma_2(\epsilon)+\Sigma_3(\epsilon),$$

$$\Sigma_1(\epsilon)=\frac{3U^2}{4\pi}\int_{-\infty}^{\infty}d\omega\,\tanh\left(\frac{\omega}{2T}\right)\mathrm{Im}G_{dR}(\omega)\chi_R(\epsilon-\omega),$$

$$\Sigma_2(\epsilon)=\frac{3U^2}{4\pi}\int_{-\infty}^{\infty}d\omega\,\tanh\left(\frac{\omega}{2T}\right)G_{dR}(\epsilon-\omega)\mathrm{Im}\chi_R(\omega), \quad (12)$$

$$\Sigma_3(\epsilon)=\frac{3U^2}{2\pi}\int_{-\infty}^{\infty}d\omega\,\mathrm{csch}\left(\frac{\omega}{T}\right)G_{dR}(\epsilon-\omega)\mathrm{Im}\chi_R(\omega).$$

III. APPROXIMATION SCHEME

Our goal is to solve simultaneously Eqs. (8), (9), (11), and (12). The first step is to replace $\chi(\omega)$ by a simple, parametrized function. This was done by Levine *et al.*,[3] for the purpose of analytically continuing $\Sigma(\epsilon)$ from the imaginary axis points where it had been computed numerically to $\epsilon=0$. They found that their calculation of $\Sigma(0)$ based on the approximate χ agreed very well with the results of strictly numerical analytic continuation. The agreement they found is our primary argument for using the approximate χ in the broader context of the present paper. However, for completeness, we will repeat the arguments on which this approximation is based.

Equation (8) implies that $\mathrm{Re}\chi_0(\omega)<1/U$; χ can be large only when the denominator in this equation is close to zero. Thus $\chi(\omega)$ can be a rapidly varying function of ω while $\chi_0(\omega)$ is varying only slowly. We expect $\mathrm{Re}\chi_0$ to be maximum at $\omega=0$, and so we expand[12]

$$\chi_0(\omega)\approx\chi_0(0)+\omega\left.\frac{d\chi_0}{d\omega}\right|_{\omega=0}. \quad (13)$$

From Eq. (9), we can easily show

$$\chi_0(0)=-\frac{1}{2\pi}\,\mathrm{Im}\int_{-\infty}^{\infty}d\epsilon\,\tanh\left(\frac{\epsilon}{2T}\right)[G_{dR}(\epsilon)]^2. \quad (14)$$

We can also show directly

$$\left.\frac{d\chi_0}{d\omega}\right|_{\omega=0}=-\frac{i}{\pi}\int_{-\infty}^{\infty}d\epsilon\,\tanh\left(\frac{\epsilon}{2T}\right)\mathrm{Im}G_{dR}(\epsilon)\frac{d}{d\epsilon}\mathrm{Im}G_{dR}(\epsilon)$$

$$=\frac{i}{2\pi}\int_{-\infty}^{\infty}d\epsilon[\mathrm{Im}G_{dR}(\epsilon)]^2\frac{d}{d\epsilon}\tanh\left(\frac{\epsilon}{2T}\right). \quad (15)$$

Suppose the minimum energy over which $G_d(\epsilon)$ can vary is T or larger. Then we can replace the tanh in Eq. (15) by a step function and make at most an error in the numerical coefficient, so

$$\left.\frac{d\chi_0}{d\omega}\right|_{\omega=0}\approx\frac{i}{\pi}[\mathrm{Im}G_d(0)]^2. \quad (16)$$

Substituting Eq. (13) in Eq. (8) and keeping only the real part of χ_0 in the numerator, we find[12]

$$\chi(\omega)\approx ic/(\omega+iT_s). \quad (17)$$

The parameter T_s can be interpreted as the width of the local spin fluctuation spectrum. We will not give explicit expressions for c and T_s until we have solved for G_d.

The exact χ must fall off more rapidly than $1/\omega$ at large ω. The energy at which the asymptotic behavior sets in is of the order of the width of $\mathrm{Im}G_d$. The expression in Eq. (17) will always appear in integrals where something else cuts the integrand off at these energies, so the error caused by the incorrect asymptotic behavior of this approximate χ should not be large.

Next, let us examine the three terms in the self-energy given in Eq. (12). We must keep in mind that $\mathrm{Im}G_d(\epsilon)$ is even and $\mathrm{Re}G_d(\omega)$ is odd about $\omega=0$ as a result of our choice of ϵ_d, Eq. (3), and that χ is to be replaced by the approximate form in Eq. (17).

The key term in Σ is Σ_1. For small T and T_s, it will be imaginary and logarithmically singular near $\epsilon=0$.[13] $\Sigma_2(\epsilon)$ must be slowly varying compared to Σ_1, since ϵ appears in the argument of G_d instead of χ. From the relation between G_d and the t matrix for conduction electron scattering, we can prove that $\mathrm{Im}G_d$ is bounded by $1/\Delta$. Therefore, G_d cannot have any isolated polelike singularities with residue of order unity on its nonphysical sheet closer to the branch cut than $-i\Delta$, and since we are supposing $T_s\ll\Delta$, our assertion is proved. From symmetry we can prove

$$\Sigma_1(0)+\Sigma_2(0)=0. \quad (18)$$

Therefore, we will approximate Σ_2 by a constant chosen to satisfy the exact Eq. (18).

[12] Such an expression for the local state susceptibility was introduced for the unrenormalized RPA by P. Lederer and D. L. Mills, Solid State Commun. **5**, 131 (1967).

[13] The existence of a logarithmic term in an unrenormalized RPA study of the Anderson model was shown by N. Rivier and M. J. Zuckermann, Phys. Rev. Letters **21**, 904 (1968). The related rapid variation of the real self-energy at $\epsilon=0$ was noted in the unrenormalized RPA by P. Lederer and D. L. Mills, *ibid.* **20**, 1036 (1967).

$\Sigma_3(\epsilon)$ must be small compared to the logarithmic terms because the $\operatorname{csch}(\omega/T)$ in the integrand cuts it off at $\omega \approx T$. Thus Σ_3 can only be important at $\epsilon=0$, where the large term Σ_2 is canceled by the rapidly varying term Σ_1. We will replace it by a constant equal to its value at $\epsilon=0$. Furthermore, we will neglect the ω dependence of G_d in the integration region, in keeping with our previously invoked supposition that G_d cannot vary appreciably on a range of order T. The expression we shall use is then

$$\Sigma_3(\epsilon) \approx \frac{3U^2c}{2\pi} G_d(0) \int_{-\infty}^{\infty} d\omega \operatorname{csch}\left(\frac{\omega}{T}\right) \frac{\omega}{\omega^2+T_s^2}. \quad (19)$$

The integral λ in Eq. (19) can be evaluated in terms of the digamma function ψ,

$$\lambda = 2\psi(T_s/\pi T) - 2\psi(T_s/2\pi T) - \pi T/T_s - 2\ln 2. \quad (20)$$

By examining the limits of large and small T_s/T, we find that λ can be replaced to a good approximation by the interpolating function

$$\lambda \approx \pi^2 T^2/T_s(2T_s+\pi T). \quad (21)$$

The approximations made up to this point have been based on the principle of exploiting the general properties of the functions involved to simplify the expressions with which we must deal. Our two final steps seem purely gratuitous in this context since they do not simplify anything. They are necessary to bring Dyson's equation into a form which can be solved by known techniques.

Let us substitute Eq. (17) for χ in Eq. (12) for Σ_1,

$$\Sigma_1(\epsilon) = i\frac{3U^2c}{4\pi} \int_{-\infty}^{\infty} d\omega \tanh\frac{\omega}{2T} \operatorname{Im} G_{dR}(\omega) \frac{1}{\epsilon-\omega+iT_s}. \quad (22)$$

$\Sigma_1(\epsilon)$ is the only term we have kept which can give $G_d(\epsilon)$ nontrivial structure. It is clear from Eq. (22) that the singularity of $\Sigma_1(\epsilon)$ closest to the physical sheet must lie at least $-iT_s$ below the branch cut along the real axis. Thus the minimum width we expect to find in the structure of $\operatorname{Im} G_d$ (on the real axis) is of order T_s. As $T_s \to 0^+$, the sharpest input structure comes from $\tanh(\omega/2T)$. Either the tanh or the iT_s serves to cut off the logarithmic divergence of the integral in Eq. (22) with $\epsilon=0$. It proves to be advantageous to replace Eq. (22) with a truly singular integral operator, and cause the tanh to take full responsibility for cutting off the logarithmic integral,

$$\Sigma_1(\epsilon) \approx i\frac{3U^2c}{4\pi} \int_{-\infty}^{\infty} d\omega \tanh\left(\frac{\omega}{2\tilde{T}}\right) \frac{1}{\epsilon-\omega+i\delta} \operatorname{Im} G_{dR}(\omega). \quad (23)$$

We have introduced the effective temperature $\tilde{T}$, whose purpose is to represent the width due to both T and T_s.

The preceding step cannot be accepted as a good approximation at this point. Using Eq. (23), it is possible that the integral equation for G_d could bypass the external source of structure, $\tanh(\omega/2\tilde{T})$, and bootstrap sharper structure into $\Sigma(\epsilon)$. With the original operator, T_s is an absolute lower bound on real-axis structure. Thus Eq. (23) can be judged acceptable only if the solution it leads to is consistent with this property of the original operator. We shall see later that this is the case.

The choice of $\tilde{T}$ is somewhat arbitrary. A reasonable basis for this choice is to require Eqs. (22) and (23) to yield similar results when $\operatorname{Im} G_d$ is replaced by some simple function, say a constant between $-U$ and U, and zero elsewhere. This gives, as the best choice,

$$\ln\tilde{T} = \ln T + \psi(\tfrac{1}{2} + T_s/2\pi T) - \psi(\tfrac{1}{2}), \quad (24)$$

where ψ is the digamma function. From the asymptotic expansion of Eq. (24), we can find the simple interpolating function

$$\tilde{T} = T + 1.13T_s. \quad (25)$$

The approximate operator in Eq. (23) is still not quite in the form we want. We wish to add to $\Sigma(\epsilon)$ the expression

$$\Sigma'(\epsilon) \equiv -\frac{3U^2c}{4\pi} \int_{-\infty}^{\infty} d\omega \tanh\left(\frac{\omega}{2\tilde{T}}\right) \frac{1}{\epsilon-\omega+i\delta} \operatorname{Re} G_d(\omega). \quad (26)$$

This integral is zero at $\epsilon=0$, since $\operatorname{Re} G_d$ is odd. It is not expected to have logarithmic singularities at any ϵ, and should be small compared to the large constant Σ_2. Furthermore, the sign of $\operatorname{Re}\Sigma'(\epsilon)$ will be such that it cannot introduce any spurious zeros in $\operatorname{Re} G_d^{-1}$. Therefore, we will replace Eq. (23) by

$$\Sigma_1(\epsilon) \approx -\frac{3U^2c}{4\pi} \int_{-\infty}^{\infty} d\omega \tanh\left(\frac{\omega}{2\tilde{T}}\right) \frac{1}{\epsilon-\omega+i\delta} G_{dA}(\omega), \quad (27)$$

where G_{dA} is the advanced Green's function.

The rather tedious arguments in this section can be summarized briefly: We approximated the d-state spin fluctuation propagator by a function with a single pole, then identified a logarithmically divergent term in the d-state self-energy, treated it correctly, and replaced the more slowly varying terms by constants. The width of the spin fluctuation spectrum T_s and the thermal smearing of the Fermi surface were lumped into a single effective temperature $\tilde{T}$.

IV. SOLUTION OF DYSON'S EQUATION

Substituting the approximated self-energy into Eq. (11), we obtain the following expressions for the retarded and advanced d-state Green's functions:

$$G_{dR}(\epsilon) = 1/\Phi_1^+(\epsilon), \quad (28)$$

$$G_{dA}(\epsilon) = 1/\Phi_2^-(\epsilon), \quad (29)$$

$$\Phi_1^{\pm}(\epsilon)=\epsilon+ia-\Sigma_2+\int_{-\infty}^{\infty}d\omega\frac{1}{\epsilon-\omega\pm i\delta}\xi(\omega)G_{dA}(\omega)\,, \quad (30)$$

$$\Phi_2^{\pm}(\epsilon)=\epsilon-ia-\Sigma_2^{*}+\int_{-\infty}^{\infty}d\omega\frac{1}{\epsilon-\omega\pm i\delta}\xi(\omega)G_{dR}(\omega)\,. \quad (31)$$

In the above, a includes the constant terms Δ and Σ_3, the Σ_2 term cancels the integral at $\epsilon=0$ as required by Eq. (18), and

$$\xi(\omega)=(3U^2c/4\pi)\tanh(\omega/2\tilde{T})\,.$$

The functions Φ_1^- and Φ_2^+ introduced in Eqs. (30) and (31) have no physical significance but will be needed in finding the solution.

Equations (28) and (29) formally resemble another set of nonlinear singular integral equations derived by the author from an approximate treatment of the *s-d* exchange model.[14] Those equations were solved exactly using complex variable techniques.[15,16] Although there are many important differences, the same methods work here.

From Eqs. (30) and (31), we see that Φ_1 and Φ_2 can be considered functions of a complex variable z ($\mathrm{Re}z=\epsilon$) which are analytic in the finite z plane except for branch cuts along the real axis. Their discontinuities across the cuts are

$$\Phi_1^{+}-\Phi_1^{-}=-2\pi i\xi G_{dA}\,, \quad (32)$$

$$\Phi_2^{+}-\Phi_2^{-}=-2\pi i\xi G_{dR}\,, \quad (33)$$

where the argument ϵ is understood everywhere. Substituting Eqs. (28) and (29) in the above, we find

$$(\Phi_1^{+}-\Phi_1^{-})\Phi_2^{-}=-2\pi i\xi\,, \quad (34)$$

$$(\Phi_2^{+}-\Phi_2^{-})\Phi_1^{+}=-2\pi i\xi\,. \quad (35)$$

If we add these equations, the result is

$$\Phi_1^{+}\Phi_2^{+}-\Phi_1^{-}\Phi_2^{-}=-4\pi i\xi\,. \quad (36)$$

The product $\Phi_1\Phi_2$ must also be analytic as a function of z except for a real-axis branch cut. That it must diverge as z^2 at infinity, and that it cannot contain a term diverging as z at infinity are easily shown from Eqs. (30) and (31). Its value at $z=0$ is known, and Eq. (36) gives its discontinuity across the branch cut. The above properties uniquely specify the function. We obtain the desired discontinuity using the digamma function, since[17]

$$\mathrm{Im}\psi(\tfrac{1}{2}\pm iy)=\pm\tfrac{1}{2}\pi\tanh\pi y\,. \quad (37)$$

Adding the needed second-order polynomial,

$$\Phi_1^{\pm}(\epsilon)\Phi_2^{\pm}(\epsilon)\equiv X^{\pm}(\epsilon)=\epsilon^2+a^2+(3U^2c/\pi)[\psi(\tfrac{1}{2}\pm\epsilon/2\pi i\tilde{T})-\psi(\tfrac{1}{2})]\,. \quad (38)$$

The next step in the solution is to solve Eq. (38) for $\Phi_2^-(\epsilon)$ and substitute the result in Eq. (34),

$$(\Phi_1^{+}-\Phi_1^{-})(X^{+}/\Phi_1^{-})=-2\pi i\xi=\tfrac{1}{2}(X^{+}-X^{-})\,. \quad (39)$$

Simple algebra yields

$$\Phi_1^{+}/\Phi_1^{-}=(X^{+}+X^{-})/2X^{-}\equiv H\,. \quad (40)$$

Equation (40) now has the form of the thoroughly studied Riemann-Hilbert boundary problem.[16] We can prove that the index[16] is zero by the method used previously.[15] The most general solution of Eq. (40) which behaves as required by Eq. (30) at infinity is

$$\Phi_1^{\pm}(\epsilon)=(\epsilon+ib)\exp\left(\frac{-1}{2\pi i}\int_{-\infty}^{\infty}d\omega\frac{\ln H(\omega)}{\epsilon-\omega\pm i\delta}\right). \quad (41)$$

The constant b can be determined by requiring that $\Phi_1^{+}(\epsilon=0)=ia$. This is a key step in determining the properties of the solution, and we will go through it in detail. The equation for b is

$$ia=ib\exp\left(\frac{-1}{2\pi i}\int_{-\infty}^{\infty}d\omega\frac{1}{-\omega+i\delta}\ln\frac{X^{+}(\omega)+X^{-}(\omega)}{2X^{-}(\omega)}\right). \quad (42)$$

Let us consider just the part of the integral in Eq. (42) involving $\ln X^-$. Since X^- is analytic in the lower half complex plane, we can deform the contour into the lower half-plane without fear of crossing any singularities unless X^- has zeros, which would be branch points of the ln. Examining Eq. (38), we see that X^- has exactly one zero on the negative imaginary axis. We will define this zero as $-ib_0$. The integrand of

$$\int_{-\infty}^{\infty}d\omega\frac{1}{-\omega+i\delta}\ln\frac{\omega^2+b_0^2}{X^{-}(\omega)} \quad (43)$$

has no singularities in the lower half-plane and converges at infinity more rapidly than $1/\omega$, so the integral is zero.

Substituting this result in Eq. (42),

$$a=b\exp\left(\frac{-1}{2\pi i}\int_{-\infty}^{\infty}d\omega\frac{1}{-\omega+i\delta}\ln\frac{X^{+}(\omega)+X^{-}(\omega)}{2(\omega^2+b_0^2)}\right). \quad (44)$$

The ln in Eq. (44) is real and an even function of ω, so the principal value part of the integral vanishes and only the δ function part contributes,

$$a=b\{[X^{+}(0)+X^{-}(0)]/2b_0^2\}^{1/2}=ba/b_0\,. \quad (45)$$

Therefore, $b=b_0$, and the solution of our integral equation is completely determined.

[14] D. R. Hamann, Phys. Rev. **158**, 570 (1967).

[15] P. E. Bloomfield and D. R. Hamann, Phys. Rev. **164**, 856 (1967).

[16] The theory of the solution of linear singular integral equations by these techniques is given by N. I. Muskhelishvilli, in *Singular Integral Equations*, translated by J. R. M. Radok (P. Noordhoff, Ltd., Groningen, The Netherlands, 1953).

[17] P. J. Davis, in *Handbook of Mathematical Functions*, edited by M. Abramowitz and I. A. Stegun (Dover Publications, Inc., New York, 1965), p. 259.

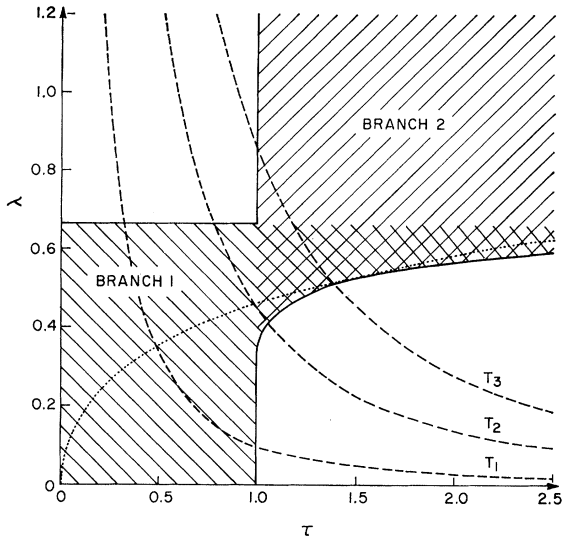

FIG. 3. Diagram of the λ-τ plane. The cross-hatched regions represent areas in which each branch of Eq. (53) can correspond to a physically permissible solution. The dashed curves show the restriction placed on the solution by Eq. (21) for several temperatures $T_1<T_2<T_3$. The dotted curve is the trajectory of an actual solution as a function of temperature.

To complete the solution of the entire problem, we should now substitute G_d, the inverse of Eq. (41), into Eqs. (14) and (16) and determine the parameters in the approximate susceptibility function self-consistently. A very helpful further simplification is possible, however. The argument showing that Eq. (43) is zero is equally valid if the singular factor has some nonzero ϵ, and we can use it to rewrite Eq. (41) and hence G_d as

$$G_{dR}(\epsilon)=\frac{1}{\epsilon+ib}\exp\left(\frac{1}{2\pi i}\int_{-\infty}^{\infty}\frac{d\omega}{\epsilon-\omega+i\delta}\ln\frac{\mathrm{Re}X^{+}(\omega)}{\omega^2+b^2}\right). \quad (46)$$

Now ω^2+b^2 can be considered a polynomial approximant to $\mathrm{Re}X^{+}(\omega)$, so we expect the ln in Eq. (46) to be small except near $\omega=0$, where X varies rapidly. (As we will see, b is a large energy, of order U.) In fact, we expect the entire exponential factor to be relatively unimportant except at small ϵ. In the integral of Eq. (14), the factor $\mathrm{Im}(G_d^2)$ goes to zero at $\epsilon=0$, so the exact value of G_d in the small ϵ region should not be important. Therefore, we will drop the exponential in this application, and use

$$\chi(0)\approx-\frac{1}{2\pi}\mathrm{Im}\int_{-\infty}^{\infty}d\epsilon\left(\tanh\frac{\epsilon}{2T}\right)\frac{1}{(\epsilon+ib)^2}$$
$$\approx 1/\pi b. \quad (47)$$

This step has been checked by numerical calculation, and we find that the error introduced is of order Δ^2/U^3.

In the notation of this section, the other susceptibility parameter is

$$\mathrm{Im}\frac{dX_0}{d\omega}\bigg|_{\omega=0}=\frac{1}{\pi a^2}. \quad (48)$$

V. SELF-CONSISTENT SOLUTION

The parameters introduced at various points throughout the preceding portion of the paper can now be collected. For the susceptibility parameters, we find from Eqs. (8), (13), (17), (47), and (48)

$$c=a^2/Ub, \quad (49)$$

$$T_s=(\pi a^2/U)(1-U/\pi b). \quad (50)$$

The single-particle hopping Δ and scattering by thermally excited spin fluctuations give the zero-energy value of G_d^{-1} through Eqs. (11), (19), (21), (28), (30), and (49),

$$a=\Delta/[1-\lambda(3U/2\pi b)], \quad (51)$$

where

$$\lambda=\pi^2T^2/T_s(2T_s+\pi T). \quad (21)$$

The final equation which is needed is that defining b, the zero of X^{-}. Since $b\gg\tilde{T}$ for any of the assumptions to be valid, we can use the asymptotic form of the digamma function in Eq. (38). Incorporating Eqs. (24) and (49) yields

$$X^{-}(-ib)=-b^2/a^2+1+(3U/\pi b)[\ln(b/2\pi T)-\psi(\tfrac{1}{2}+T_s/2\pi T)]$$
$$=0. \quad (52)$$

For given values of Δ, U, and T, Eqs. (50), (51), (21), and (52) must be solved simultaneously. This is not as difficult as it may appear. First, we pick a trial value for T_s. After computing λ from Eq. (21), Eqs. (50) and (51) are solved for b algebraically,

$$b=\left(\frac{U}{\pi}\right)\frac{(1-3\lambda\tau)\pm[1-6\tau\lambda(1-3\lambda/2)]^{1/2}}{2(1-\tau)}, \quad (53)$$

where

$$\tau=T_sU/\pi\Delta^2. \quad (54)$$

The upper sign in Eq. (53) will be denoted branch 1, and the lower sign branch 2. Obtaining a from Eq. (51), $X(-ib)$ is computed using Eq. (52) and compared to zero. Thus we really only solve a transcendental equation in one variable, T_s.

Choosing the proper branch of Eq. (53) requires care. In Fig. 3, the regions in the τ-λ plane in which each branch can give physically permissible solutions are shown by the cross-hatched areas. The solution must lie on a τ-λ curve computed from Eq. (21). Such curves for three temperatures $T_1<T_2<T_3$ are shown in Fig. 3 as dashed lines. The search procedure along each λ-τ curve must differ depending on its position in the cross-hatched areas. Both branches of Eq. (53) must be examined in the overlap area.

The trajectory of an actual solution is shown by the dotted line. It starts at low T at the origin. For a wide temperature range (several decades) it traverses the branch 1 region, and $T_s\sim T$, since $\lambda\sim 1$. It crosses into the overlap region at a rather high temperature,

$T\sim\Delta^2/U$, and approaches the lower boundary, on which the square root in Eq. (53) is zero and both branches are identical. As the temperature increases further, it switches to branch 2 and pulls above the boundary. At extremely high temperatures, $T\sim\Delta$, it moves out of the overlap region into the branch 2 only region, but this cannot be shown on the scale of Fig. 2.

Some important results can be extracted without computation. For very low T, we will assume $T\ll T_s\ll\Delta<U$. Then $a\approx\Delta$, $b\approx U/\pi$, and Eq. (52) reduces to

$$3\ln(U/\pi T_{s0})\sim(U/\pi\Delta)^2-1, \tag{55}$$

so

$$T_{s0}\sim(U/\pi)e^{-(1/3)(U/\pi\Delta)^2+1/3}. \tag{56}$$

This is the most important result of the calculation. λ will remain close to zero and T will be negligible in Eq. (52) until $T\approx T_{s0}$, so the solution is temperature-independent below T_{s0}. The zero-frequency susceptibility at these temperatures is

$$\chi=(\Delta/U)^2(\pi/T_{s0}). \tag{57}$$

The resistivity $R=\Delta/a$ in unitarity-limit units and is 1 as $T\to 0$. For finite $T<T_s$, Eqs. (21) and (51) show that

$$R\approx 1-(3\pi^2/4)(T/T_{s0})^2. \tag{58}$$

For $T_{s0}<T\ll\Delta^2/U$, Eq. (53) indicates that b remains $\approx U/\pi$. Equation (51) then requires $\lambda<\frac{2}{3}$, so we infer from Eq. (21) that $T_s>T$. If we now consider the strongly magnetic case, $U/\Delta\gg 1$, the digamma function and the 1 in Eq. (52) should be negligible, so

$$(U/\pi a)^2\approx 3\ln(U/T). \tag{59}$$

Substituting the leading term from Eq. (56), the resistivity in this regime can be written

$$R\approx[1-3(\pi\Delta/U)^2\ln(T/T_{s0})]^{1/2}. \tag{60}$$

For an initial portion of the temperature range considered here, the square root can be expanded and the resistivity will vary logarithmically with a slope proportional to $(\Delta/U)^2$. In this region, we can work backwards from a to λ to T_s, and obtain for the susceptibility

$$\chi\approx\pi\left(\frac{\Delta}{U}\right)^3\left(\frac{1}{T}\right)\left[2\ln\left(\frac{T}{T_{s0}}\right)\right]^{1/2}. \tag{61}$$

For sufficiently high T, $T\gg\Delta^2/U$, we can neglect the logarithmic terms in the self-energy, Σ_1 and Σ_2, and just keep Σ_3. Under these conditions, the theory reduces to that of Ref. 1, except for the fact that we have treated Σ_3 as a constant rather than a constant times $G_d(\epsilon)$. This changes the broadened square-root function for $G_d(\epsilon)$ found in Ref. 1 into a Lorentzian, but leads to essentially the same result for the susceptibility,

$$\chi\sim 1/T. \tag{62}$$

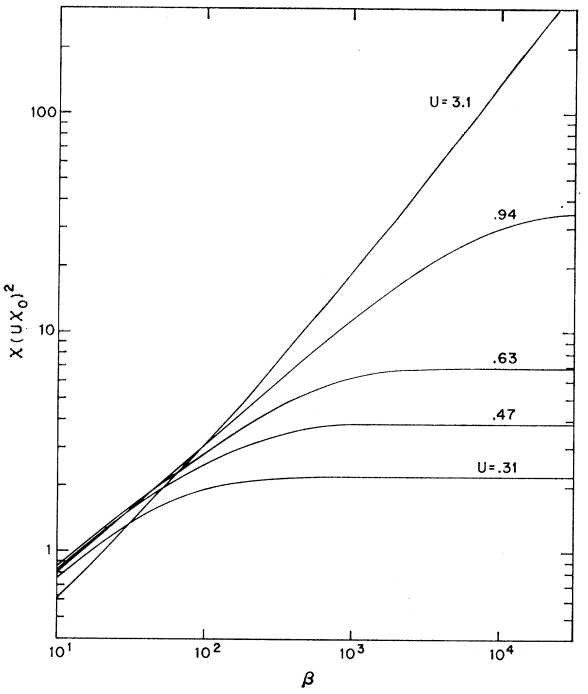

FIG. 4. Susceptibility times $(U\chi_0)^2$ in reciprocal energy units versus $\beta=1/T$ for $\Delta=0.1$ and values of U as indicated. These results may be compared with Fig. 1 of Ref. 2.

The resistivity is again constant in this regime,

$$R\sim\pi\Delta/U. \tag{63}$$

The self-consistency equations have been solved numerically to facilitate comparison with the published results of the numerical integral equation solution. In so doing, the factor $\frac{3}{2}$ in Eq. (10) was changed back to $\frac{3}{4}$. In addition, we have plotted $\chi(U\chi_0)^2$ rather than χ, since this is the quantity plotted as χ in Ref. 2.[18] We have chosen values of U which are simple multiples of the critical $U=\pi\Delta$, but are close to (where not equal to) the values for v used in Refs. 2 and 3. The resistivity and "susceptibility" are plotted in Figs. 4 and 5.

The spectral density $\mathrm{Im}G_d(\epsilon)$ is plotted in Fig. 6 for two temperatures. Note that the spectrum is characterized by just two energies, T_s and U. (The factor was $\frac{3}{2}$ for these plots.) It is clear that our assumptions about the width of the structure of G_d are self-consistently satisfied.

VI. CONCLUSIONS

The qualitative behavior of the resistivity and susceptibility shown in Figs. 4 and 5 is sufficiently similar to that found from the numerical solution[2,3] to support the approximation scheme.

The most easily identified error preventing better quantitative agreement is the neglect of the energy dependence of Σ_2 and Σ_3 at large ϵ. We can reasonably

[18] M. Levine (private communication).

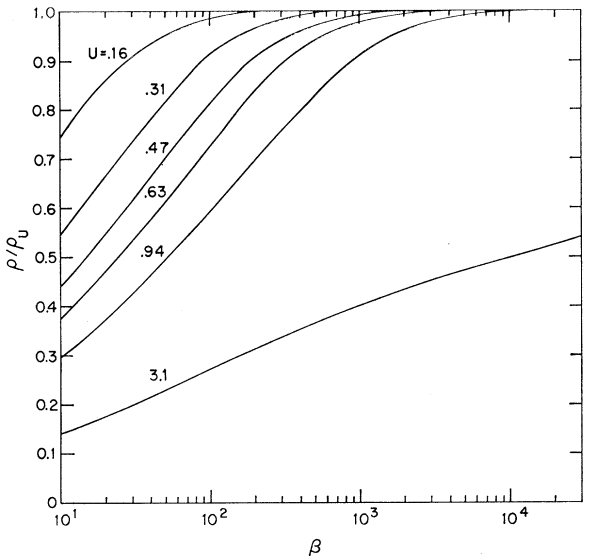

FIG. 5. Resistivity in unitarity-limit units versus $\beta=1/T$ for $\Delta=0.1$ and U as indicated. These results may be compared to Figs. 1 and 2 of Ref. 3.

suppose that if this approximation were improved, the characteristic temperature would continue to be given by an expression of the type

$$b^2/\Delta^2=1+3\ln(U/T_{s0}). \tag{64}$$

The energy b would still characterize the over-all width of the G_d spectrum. However, since this spectrum would no longer be Lorentzian at large ϵ, the numerical coefficient α in $\chi_0(0)=\alpha/b$ would be something other than $1/\pi$. The relation $U\chi(0)\approx 1$ must hold, so

$$T_{s0}\approx Ue^{-(1/3)(\alpha U/\Delta)^2+1/3} \tag{65}$$

would replace Eq. (54). Thus we must accept an uncertainty in the numerical coefficient of the exponential dependence of the characteristic temperature on $(U/\Delta)^2$ as a consequence of the simplicity of our approximation. This fact in no way invalidates the elucidation of the behavior of the coupled integral equations. We believe that the results are adequate to evaluate the basic physical approximation—the RRPA.

The RRPA is the only treatment of the Anderson model which has been carried out for all temperatures in the strongly interacting case and gives anything resembling experimentally observed dilute alloy behavior.[19] The major failure of the theory in this respect is the magnitude of the susceptibility. If we attempt to fit the RRPA result with a Curie-Weiss law at low T, we see from Eq. (57) that the Curie constant will be of order $(\Delta/U)^2$, while experimentally it is of order one.

A more serious failing of the RRPA is found on comparison with various studies of the Anderson model which treat U exactly and expand in Δ.[7,8] These studies find results which are parallel, within the Schrieffer-Wolff transformation,[9] to those obtained from the s-d exchange model. With our parameters, the characteristic energy (Kondo temperature) given by these calculations is

$$T_K\approx Ue^{-\pi U/8\Delta}. \tag{66}$$

In the large U/Δ region where these results are valid, this energy is greater by an enormous factor than T_{s0}, the characteristic energy of the RRPA, Eq. (63). We conclude that the RRPA omits important classes of diagrams which would produce structure with this larger characteristic energy.

The most complete treatment of the s-d exchange model, based on an approximation formulated rather differently by several authors,[14,20–22] leads to fairly satisfactory results for the resistivity and specific heat.[15] (It does not yield satisfactory results for the low-temperature susceptibility.[23]) One of the notable characteristics of the solution given by this approximation is that the properties depend on the logarithm of T all the way down to $T=0$, so the point $T=0$ is highly singular. The obvious cause is that the spin-flip process involves exactly zero energy in this treatment. In the RRPA, the ln functions are cut off by the width of the spin fluctuation propagator, and the various properties depend only algebraically on (T/T_{s0}) as $T\to 0$.

We might speculate that the spin-lifetime and Kondo-effect processes are complementary, and that a theory properly including both might possess two distinct characteristic temperatures. This speculation is con-

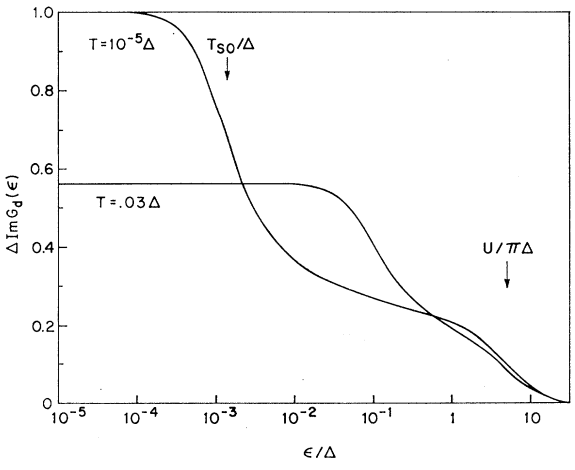

FIG. 6. Spectral density versus energy for $U/\pi\Delta=5$, at two temperatures, $T=10^{-5}\Delta$ and $T=0.03\Delta$.

[19] M. D. Daybell and W. A. Steyert, Rev. Mod. Phys. **40**, 380 (1968).

[20] H. Suhl, in *Proceedings of the International School of Physics "Enrico Fermi," Course 37* (Academic Press Inc., New York, 1967).

[21] Y. Nagaoka, Phys. Rev. **138**, A1112 (1965).

[22] A. A. Abrikosov, Zh. Eksperim. i Teor. Fiz. **48**, 990 (1965) [English transl.: Soviet Phys.—JETP **21**, 660 (1965)]; Physics **2**, 5 (1965); **2**, 61 (1965).

[23] J. Zittartz, Z. Physik **217**, 155 (1968).

travened by Dworin's analysis of the heirarchy of equations of motion for Anderson's model.[24] He derived an integral equation for G_d bearing a resemblance to the integral equation occurring in the aforementioned treatment of the *s-d* exchange model.[16] However, the key integral operator is not singular, but broadened by a finite imaginary term which could correspond to our T_s. Dworin estimates that this term is of *the same* order as the Kondo temperature.

The other major criticism which can be leveled against the RRPA on the basis of equation-of-motion calculations is its failure to produce a spectral density with peaks at ϵ_d and ϵ_d+U.[24,25] The RRPA simulates this structure only to the extent that the spectral density is spread over a range of order U. It is not clear to what extent the details of the spectrum at large energy effect the low-energy structure associated with the Kondo effect.

ACKNOWLEDGMENTS

The author acknowledges stimulating discussions with H. Suhl, W. F. Brinkman, J. A. Appelbaum, M. Levine, and R. A. Weiner.

[24] L. Dworin, Phys. Rev. **164**, 841 (1967).

[25] B. Kjöllerström, D. J. Scalapino, and J. R. Schrieffer, Bull. Am. Phys. Soc. **11**, 79 (1966).

PHYSICAL REVIEW VOLUME 186, NUMBER 2 10 OCTOBER 1969

Magnetic Neutron Scattering in Dysprosium Aluminum Garnet. I. Long-Range Order*

J. C. NORVELL† AND W. P. WOLF
Yale University, New Haven, Connecticut 06511

AND

L. M. CORLISS, J. M. HASTINGS, AND R. NATHANS
Brookhaven National Laboratory, Upton, New York 11973

(Received 5 May 1969)

Magnetic long-range order has been studied in antiferromagnetic dysprosium aluminum garnet (DAG) using coherent neutron scattering to measure the sublattice magnetization in the vicinity of the critical temperature. The value of the critical exponent β in the power-law expression for the magnetization $M \sim(\Delta T)^\beta$ was found to be 0.26 ± 0.02 for the temperature range $0.0010<\Delta T_c<0.056$. This is significantly lower than the theoretical estimate of 0.312 for the three-dimensional nearest-neighbor Ising model, with which DAG is compared.

I. INTRODUCTION

THERE has recently been much interest in the study of the order-disorder phenomena that occur in magnetic systems at the critical point T_c.[1,2] In antiferromagnetics the long-range order of atomic spins that appears for $T<T_c$ gives rise to a spontaneous sublattice magnetization M, the appropriate order parameter for magnetic systems. As the temperature increases towards T_c, the long-range order decreases and vanishes at T_c, and thus the spontaneous sublattice magnetization approaches zero. The temperature dependence is characterized by the critical exponent β, which is defined[1] by

$$M \propto [(T_c-T)/T_c]^\beta \quad \text{as } T\rightarrow T_c. \tag{1}$$

The present paper (I) describes the determination of β from measurements of the magnetization below the critical point. The following paper (II) [Phys. Rev., **186**, 567 (1969)] describes the critical scattering above T_c and the evaluation of the relevant parameters γ, ν, and η.

The techniques of neutron diffraction provide an excellent tool for the investigation of these magnetic order-disorder phase transitions. The spontaneous sublattice magnetization gives rise to strong magnetic Bragg peaks that occur at reciprocal-lattice points, and thus can be rather easily measured. The scattering cross section for such a reflection is proportional to M^2 and thus 2β can be determined from a study of the temperature dependence of the intensity. Diffuse critical scattering is superimposed on these Bragg peaks, but this scattering is relatively weak except in the temperature region very close to the critical point. At lower temperatures the main difficulty in determining β is ensuring that extinction does not affect the results.

Theoretical estimates of the critical exponent β have been obtained from numerous statistical-mechanical

* Work performed under the auspices of the U. S. Atomic Energy Commission.

† Present address: Los Alamos Scientific Laboratory, Los Alamos, N. M.

[1] See, e.g., C. Domb, Advan. Phys. **9**, 149 (1960); M. E. Fisher, Rept. Progr. Phys. **30**, 615 (1967).

[2] P. Heller, Rept. Progr. Phys. **30**, 731 (1966).